

**First order perturbative calculations for a  
conducting liquid jet in a solenoid**  
**DRAFT 3**

J. Gallardo, S. Kahn, R. B. Palmer, P. Thieberger, R Weggel  
Brookhaven National Laboratory

K. McDonald  
Princeton

February 21, 2001

**Abstract**

A perturbative calculation is given of the behavior of a continuous jet of conducting fluid as it enters and leaves a solenoidal magnetic field. It is assumed that the changes in direction, jet cross section and velocity are small.

If the jet enters the field along, or close to the axis, then the induced forces are compressive and retarding. The jet slows, suffers an increase in hydrostatic pressure, and increases in diameter; later, the jet re accelerates and shrinks. As the jet leaves the field, the hydrostatic pressure becomes negative and cavitation may occur.

If the jet enters at an angle to the axis, there are, in addition, deflections and elliptical deformations of the jet.

Formulae are given for these effects and numerical values given for the example of a solenoidal field with a Gaussian axial profile.

## Contents

<b>1</b>	<b>Introduction</b>	<b>2</b>
<b>2</b>	<b>Formulae</b>	<b>2</b>
2.1	Introduction . . . . .	2
2.2	Induced azimuthal current . . . . .	3
2.3	Radial forces and Hydrostatic pressure . . . . .	4
2.4	Axial force . . . . .	4
2.5	Axial accelerations . . . . .	6
2.6	Transverse forces and deflections . . . . .	6
2.7	Induced axial current . . . . .	8
2.8	Transverse elliptical distortion . . . . .	8

2.8.1	Magnetic Forces . . . . .	9
2.8.2	Surface Tension Forces . . . . .	10
2.8.3	Magnetic and Surface Tension Forces . . . . .	11
<b>3</b>	<b>Gaussian Case</b>	<b>11</b>
<b>4</b>	<b>Early Example</b>	<b>12</b>
<b>5</b>	<b>Study 2 Example</b>	<b>13</b>
<b>6</b>	<b>Coil Design</b>	<b>17</b>
<b>7</b>	<b>Conclusion</b>	<b>19</b>

## 1 Introduction

A mercury jet, injected at an angle respect to the axis of the solenoidal field, is the current baseline solution for the Feasibility Study II[1]. The interaction of the liquid-metal jet with the strong 20 T target solenoid has as result a number of forces on the jet which potentially may affect the viability of this target.[2],[3],[4] We present here perturbative calculations which confirm the findings of previous authors.

## 2 Formulae

### 2.1 Introduction

The jet is assumed to have an initial radius  $r$ , and be traveling at a velocity  $v$ . Changes in radius, shape, direction and velocity are all assumed to be small. The angle between the jet and solenoid axes is also assumed to be small.

No viscosity  
 $r \ll L$

In the following formulae, the coordinate system is defined by the jet;  $z$  is along the direction of motion and  $r$  is perpendicular to  $z$ .

If the jet is not directed along the solenoid axis, then we also define  $y$  in a direction perpendicular to  $z$  (the jet axis) and away from the solenoid axis; and  $x$  perpendicular to  $y$  and  $z$ ; and we define a second coordinate system  $x' y' z'$ , where  $z'$  is aligned along the magnet axis. Assuming a small angle  $\theta^2 \ll 1$  then (See fig. 2.1):

$$x' \approx x$$

$$y' \approx y_0 + z \theta$$

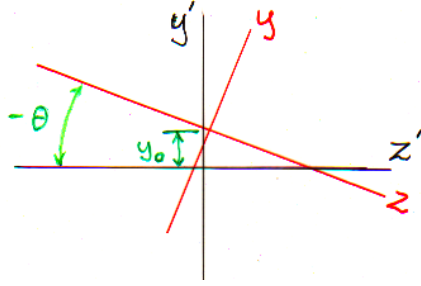


Figure 1: Schematic of the geometrical arrangement of solenoid and jet

$$r'^2 \approx r^2 + 2z y_0 \theta$$

$$z' \approx z - y_0$$

## 2.2 Induced azimuthal current

The magnetic flux through a circle of radius  $r$  perpendicular to the jet axis is

$$\Phi = \int_S dS \vec{n} \cdot \vec{B} \approx \pi r^2 B_z(x, y, z) \quad (1)$$

As a liquid metal jet passes axially down such a field at a velocity  $v = dz/dt$ , a circumferential potential will be generated[6]

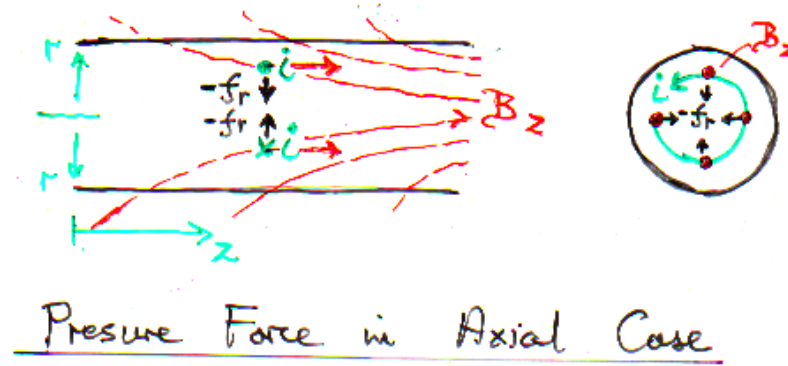
$$V \equiv \oint \vec{E} \cdot d\vec{l} = -\frac{d\Phi}{dt} = \pi r^2 v \frac{dB_z(x, y, z)}{dz} \quad (2)$$

If the metal electrical conductivity  $\sigma$  is low enough so that the resulting current has a negligible effect on the field, then the azimuthal current density  $i_\phi$  will be

$$i_\phi \approx \frac{V}{2\pi r} \sigma \quad (3)$$

$$i_\phi \approx \frac{rv\kappa}{2} \frac{dB_z(0, 0, z)}{dz} \quad (4)$$

### 2.3 Radial forces and Hydrostatic pressure



The induced radial force per unit volume ( $dr r d\phi dz$ ) is

$$f_r = B_z i_\phi \approx \frac{r}{2} v \kappa B_z \frac{dB_z}{dz} \quad (5)$$

If we assume the effects of the fields are small so that the jet radius and liquid velocities do not vary by large fractions, and if we ignore radial inertia, then the hydrostatic pressures in a jet of outside radius  $r_o$ , at radius  $r$ , will be given by

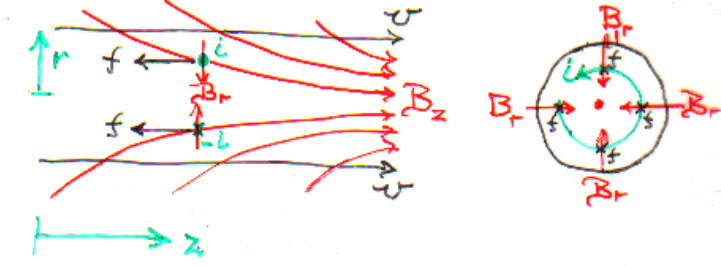
$$p(r, z) = \int_{r_o}^r -f_r dr \approx \left( \frac{r_o^2 - r^2}{4} \right) v \kappa B_z \frac{dB_z}{dz} \quad (6)$$

### 2.4 Axial force

The above hydrostatic pressure is a function of  $z$ , and gradients in it will exert axial pressures  $f_p$  on the liquid that must be added to the magnetic term  $f_z$ (hydrostatic).

$$f_p(\text{hydrostatic}) = \frac{dp(r, z)}{dz} \approx - \left( \frac{r_o^2 - r^2}{4} \right) v \kappa \frac{d}{dz} \left( B_z \frac{dB_z}{dz} \right) \quad (7)$$

To this must be added the axial forces induced directly by the fields acting on the asymuthal currents:



### Retarding Force in Axial Case

If the jet is aligned with the field axis ( $\theta = 0$ ), the radial field is given by

$$B_r(\theta = 0) \approx -\frac{r}{2} \frac{\partial B_z(0, 0, z)}{\partial z} \quad (8)$$

The induced axial force per unit volume ( $dr d\phi dz$ ) is

$$f_z(\theta = 0) = f_p(r, z) - B_r i_\phi$$

If the jet is at an angle to the magnetic axis, then there is an additional shear force:

$$f_z(\theta) = f_p(r, z) - B_y i_\phi \sin(\phi)$$

giving, in all:

$$f_z \approx -\left(\frac{r_o^2 - r^2}{4}\right) v\kappa \frac{d}{dz} \left(B_z \frac{dB_z}{dz}\right) + \frac{r^2}{4} v\kappa \left(\frac{dB_z}{dz}\right)^2 + \frac{rv\kappa}{2} B_y \frac{dB_z}{dz} \sin(\phi) \quad (9)$$

On the jet axis:

$$f_z \approx -\left(\frac{r_o^2}{4}\right) v\kappa \frac{d}{dz} \left(B_z \frac{dB_z}{dz}\right) \quad (10)$$

On the outer surface, averaged over the azimuthal angle  $\phi$ , or in the absence of a  $B_y$ :

$$f_z \approx \frac{d}{dz} \left(B_z \frac{dB_z}{dz}\right) + \frac{r^2}{4} v\kappa \left(\frac{dB_z}{dz}\right)^2 \quad (11)$$

On the outer surface, with a finite  $B_y$ , as in the case of a jet at an angle to the magnetic axis:

$$f_z \approx \frac{d}{dz} \left( B_z \frac{dB_z}{dz} \right) + \frac{r_o^2}{4} v \kappa \left( \frac{dB_z}{dz} \right)^2 + \frac{y v \kappa}{2} B_y \frac{dB_z}{dz} \quad (12)$$

and the average force of the disk of radius  $r_o$  is given by integrating the terms

$$\langle f_z \rangle \approx \frac{r_o^2}{8} v \kappa \left( \left( \frac{dB_z}{dz} \right)^2 + \frac{d}{dz} \left( B_z \frac{dB_z}{dz} \right) \right) \quad (13)$$

## 2.5 Axial accelerations

These forces will then decelerate, or accelerate layers of the fluid, thus inducing differences of liquid velocity as a function of radius

$$\frac{dv}{dz} = \frac{f}{\rho v} \quad (14)$$

$$\Delta v(r, z) = \int_{z_o}^z (f_z + f_p) \frac{1}{v \rho} dz \quad (15)$$

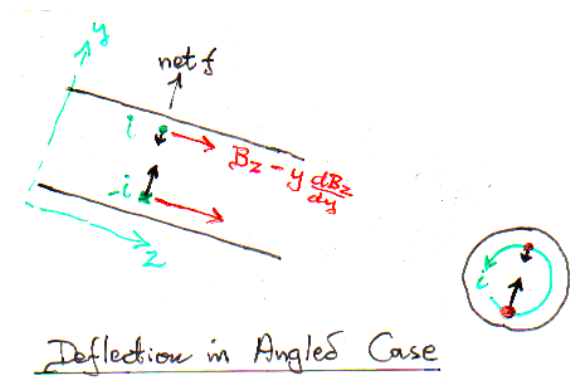
The average change in velocity is then

$$\langle \Delta v \rangle (z) = \frac{\kappa}{\rho} \frac{r_o^2}{8} \left( \int_{z_o}^z \left( \frac{dB_z}{dz} \right)^2 + \frac{d}{dz} \left( B_z \frac{dB_z}{dz} \right) dz \right) \quad (16)$$

and the radius as a function of  $z$  is

$$r(z) = r_o \left( 1 - \frac{\langle \Delta v \rangle (z)}{v} \right) \quad (17)$$

## 2.6 Transverse forces and deflections



From above, the radial force per unit volume ( $dr r d\phi dz$ ) is

$$f_r = B_z i_\phi \approx \frac{r}{2} v \kappa B_z \frac{dB_z}{dz} \quad (18)$$

If  $B_z$  varies with a transverse distance  $y$ , then the component of this radial force in the  $y$  direction is

$$f_y = f_r \sin \phi \quad (19)$$

and the net deflective force  $dF_y$  per unit length  $dz$  is

$$\frac{dF_y}{dz} = \int_0^r \int_0^{2\pi} \frac{r}{2} v \kappa \frac{dB_z}{dy} r \sin^2 \phi \frac{dB_z}{dz} r dr d\phi \quad (20)$$

$$= \frac{v \kappa}{2} \frac{dB_z}{dy} \frac{dB_z}{dz} \int_0^{2\pi} \sin^2 \phi d\phi \int_0^r r^3 dr \quad (21)$$

$$= \frac{\pi}{8} v \kappa r^4 \frac{dB_z}{dy} \frac{dB_z}{dz} \quad (22)$$

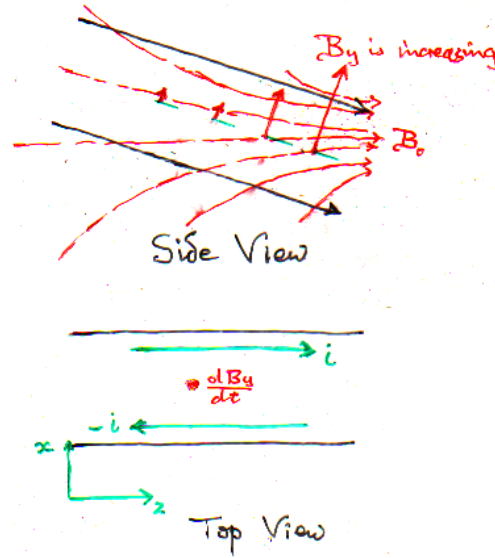
and the change in transverse velocity

$$\begin{aligned} \frac{dv_y}{dz} &= \frac{1}{v} \frac{dv_y}{dt} \\ &= \frac{\frac{dF_y}{dz} dz}{v \rho \pi r^2 dz} \\ &= \frac{\kappa r^2}{8 \rho} \frac{dB_z}{dy} \frac{dB_z}{dz} \end{aligned}$$

and the inverse radius of bend is

$$\frac{d^2 y}{dz^2} = \frac{d\theta}{dz} = \frac{\kappa r^2}{8 v \rho} \frac{dB_z}{dy} \frac{dB_z}{dz} \quad (23)$$

## 2.7 Induced axial current



Consider a transverse field component  $B_y$   
 The magnetic flux between transverse positions  $-x$  to  $x$  and  $dz$  is

$$d\Phi_y = 2x dz B_y(z) \quad (24)$$

As a liquid metal jet passes axially down such a field at a velocity  $v = dz/dt$ , axial voltage gradients will be generated

$$G = x \frac{dB_y}{dz} v \quad (25)$$

If the metal electrical conductivity  $\kappa$  is low enough so that the resulting current has a negligible effect on the field, then the axial current density  $i_z$  will be

$$i_z = G\sigma \quad (26)$$

$$i_z = xv\kappa \frac{dB_y(0,0,z)}{dz} \quad (27)$$

## 2.8 Transverse elliptical distortion

If the jet is not on the solenoid axis, the axial induced currents interacting with the transverse fields will generate distorting forces on the jet. These transverse



forces per unit volume  $dx dy dz$  are

$$f_x = i_z B_y = x v \kappa B_y \frac{dB_y}{dz} \quad (28)$$

This force will distort the cross section. Assuming that the liquid is incompressible, we must find the induced pressures and motions  $\Delta \vec{r}$  within the cross section that are driven by this force, with the constraint that the divergence of these motions is zero:

$$Div(\Delta \vec{r}) = 0$$

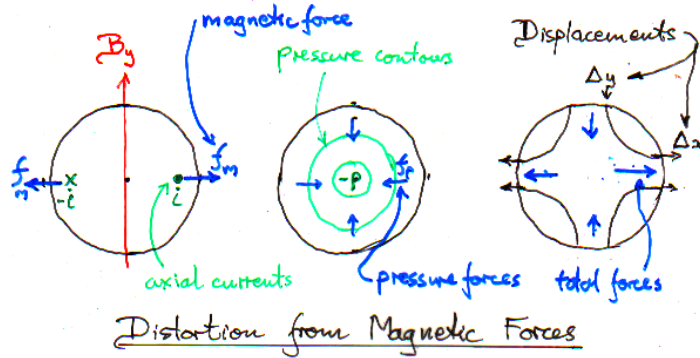
Defining

$$F_o = v \kappa B_y \frac{dB_y}{dz}$$

so that the magnet force per unit volume:

$$f_x(\text{magnetic}) = x F_o$$

### 2.8.1 Magnetic Forces



The pressure on the surface of the jet will be independent of azimuth  $\phi$ :

$$p(r_o)_{\text{circular}} = p_{\text{atm}} + T/r_o ,$$

$T$  being the surface tension. If the initial cross section is circular, we can consider pressures within the cross section:

$$p = p_o - r^2 \frac{F_o}{4}$$

where  $p_o$  is set by the constraint the above surface pressure at  $r = r_o$ . This bulk pressure will induce radial pressure forces:

$$f_r(\text{pressure}) = \frac{dp}{dr} = - \frac{r F_o}{2}$$

so

$$f_x(\text{total}) = F_o \left( x - \frac{r \cos(\phi)}{2} \right) = \frac{x F_o}{2}$$

$$f_y(\text{total}) = - \frac{F_o r \sin(\phi)}{2} = - \frac{y F_o}{2}$$

and the accelerations:

$$\frac{d^2 x, y}{dz^2} = \frac{f_{x, y}}{v^2 \rho}$$

will give displacements:

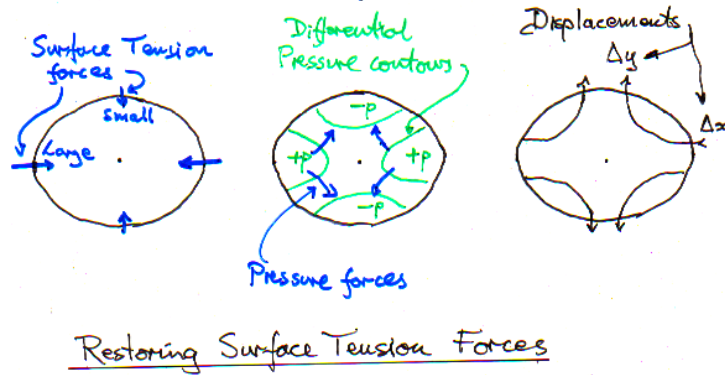
$$\Delta x = \int \int \frac{f_{x, y}}{v^2 \rho} dz^2 = x \frac{\kappa}{2 v \rho} \int \int B_y \frac{dB_y}{dz} dz^2$$

$$\Delta y = \int \int \frac{f_{x, y}}{v^2 \rho} dz^2 = -y \frac{\kappa}{2 v \rho} \int \int B_y \frac{dB_y}{dz} dz^2$$

Such motions are quadrupole ( see fig<sup>\*\*\*</sup>) and, as required, give  $Div(dx, dy) = 0$ .  
The resulting ellipticity  $\epsilon = \frac{\Delta x_o}{r_o} = - \frac{\Delta y_o}{r_o}$ :

$$\epsilon(z) = \frac{r_o \kappa}{2 v \rho} \int \int B_y \frac{dB_y}{dz} dz^2 \quad (29)$$

### 2.8.2 Surface Tension Forces



Once the cross section becomes somewhat elliptical (we consider only a small ellipticity), then the pressure at the surface is no longer independent of the asymuthal angle  $\phi$ , but is given by:

$$p(r = r_o) = p_{\text{atm}} + \frac{T}{r_o} (1 - \epsilon) \cos(2 \phi)$$

Consider, in addition to those given above for the circular case, pressures within the cross section:

$$p(x, y)_{\text{elliptical}} = p_o + \frac{T \epsilon}{r_o} (\cos^2(2 \phi) - \sin^2(2 \phi)) = p_o + \frac{T \epsilon}{r_o^3} (x^2 - y^2)$$

which has the correct values at  $r = r_o$ .

Defining

$$S_o = \frac{2 T \epsilon}{r_o^3},$$

the resulting bulk forces are:

$$f_x(\text{elliptical}) = \frac{dp}{dx} = x S_o$$

$$f_y(\text{elliptical}) = \frac{dp}{dy} = -y S_o$$

which are, once again, quadrupole forces that will generate quadrupole motions with  $\text{Div}(\vec{dr})=0$ .

$$\Delta x, \Delta y = \iint \frac{(x, -y)}{v \rho} S_o dz^2$$

### 2.8.3 Magnetic and Surface Tension Forces

Adding these surface tension displacements to the forces derived for the circular case:

$$\Delta x, \Delta y = (x, -y) \iint \left( \frac{\kappa}{2 v \rho} B_y \frac{dB_y}{dz} + \frac{2 T \epsilon}{v \rho r_o^3} \right) dz^2$$

and the resulting ellipticity  $\epsilon = \frac{\Delta x_o}{r_o} = -\frac{\Delta y_o}{r_o}$ :

$$\epsilon(z) = \iint \left( \frac{r_o \kappa}{2 v \rho} B_y \frac{dB_y}{dz} + \frac{2 T \epsilon}{v \rho r_o^3} \right) dz^2 \quad (30)$$

## 3 Gaussian Case

We can consider a field that varies as a Gaussian in  $z$ . The fields of the solenoid and coordinates are denoted with primes ( $'$ ).

The Fields in the magnet system are:

$$B'_z(r', z') \approx B_o e^{-\frac{z'^2}{2\sigma_z^2}} - \frac{1}{4} r'^2 \frac{\partial^2 B'_z(0, z')}{\partial z'^2} \quad (31)$$

$$B'_r(r', z') \approx -\frac{1}{2} r' \frac{\partial B'_z(0, z')}{\partial z'} \quad (32)$$

In the coordinate system of the jet, see Fig. 2.1, assuming a very small angle  $\theta$  then  $x' = x$ ,  $y' = y_o + z\theta$ ,  $r'^2 = r^2 + 2zy_o\theta$  and  $z' = z - y_o\theta$  and the fields are

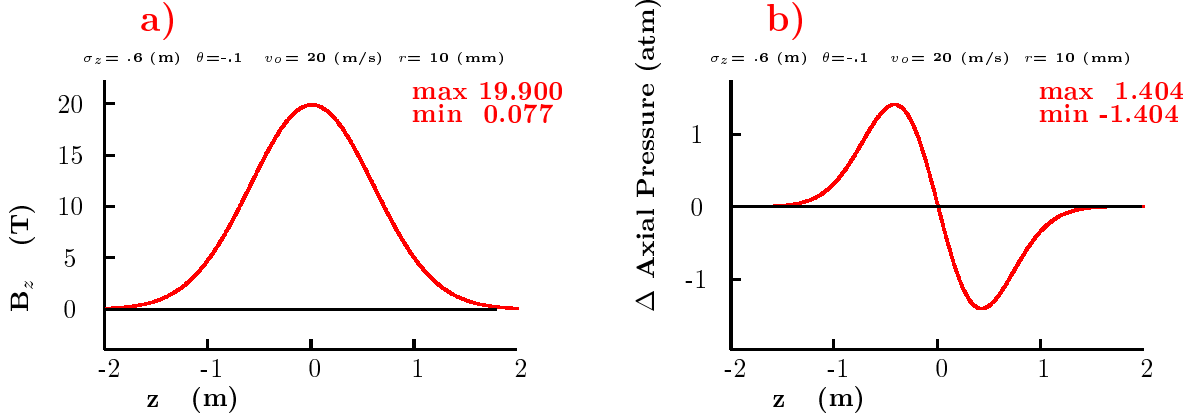
$$\begin{aligned}
B_z(x, y, z) &\approx \left[ B'_z(r', z') - \frac{1}{2}\theta y_o \frac{\partial B'_z(0, z')}{\partial z'} \right] \\
B_x(x, y, z) &\approx -\frac{1}{2}x \frac{\partial B'_z(0, z')}{\partial z'} \\
B_y(x, y, z) &\approx -\left[ \frac{1}{2}(y_o + z\theta) \frac{\partial B'_z(0, z')}{\partial z'} - \theta B'_z(r', z') \right] \\
\frac{\partial B_z(x, y, z)}{\partial z} &\approx \left[ \frac{\partial B'_z(0, z')}{\partial z'} - \frac{1}{2}y_o \theta \frac{\partial^2 B'_z(0, z')}{\partial z'^2} \right] \\
\frac{dB_y(x, y, z)}{dz} &\approx \left[ \frac{1}{2}\theta \frac{\partial B'_z(0, z')}{\partial z'} - \frac{1}{2}(y_o + z\theta) \frac{\partial^2 B'_z(0, z')}{\partial z'^2} \right] \quad (33)
\end{aligned}$$

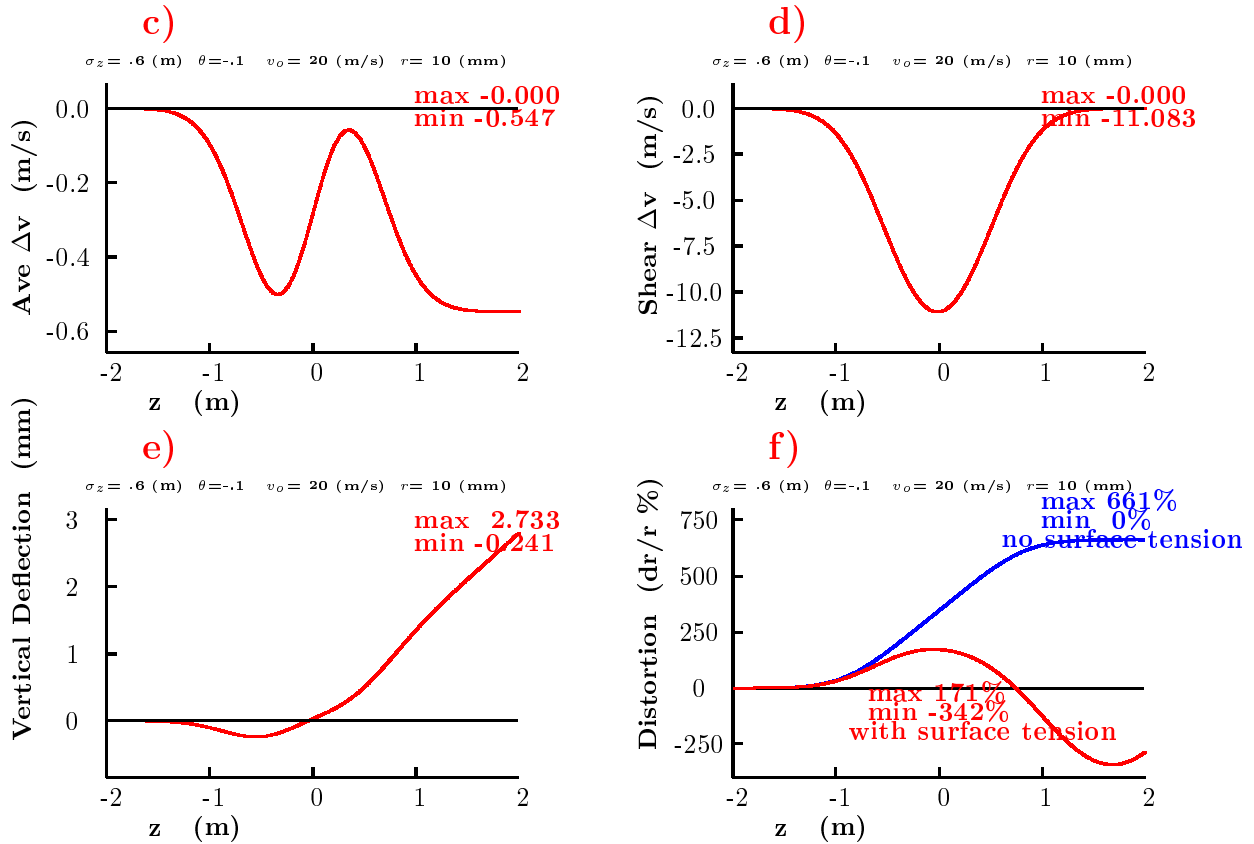
## 4 Early Example

In our earlier studies we had considered a jet entering from outside the field, with the following parameters:

$\sigma_r$	3	mm
$r_o$	10	mm
$v_o$	20	m/sec
$\theta$	100	mrads
$\sigma_z$	0.6	m

Using the above fomulae we obtain the results plotted in fig\*\*\*.





It is seen that although the deflection of the jet is small (3mm) and the average deceleration is reasonable (0.5 m/sec, yet there are several unacceptable results:

- The hydrostatic pressure falls to -1.5 atmospheres, and would require a high pressure environment to stop the jet breaking up.
- There are shear accelerations of  $\pm 11$  m/sec. leading to a 3:1 ratio of velocity across the jet.
- The calculated distortion with surface tension included is 340% (without the surface tension it is 700%), indicating that the calculation is beyond its valid region. But indicating that the jet will be badly disrupted.

Clearly these parameters are unacceptable.

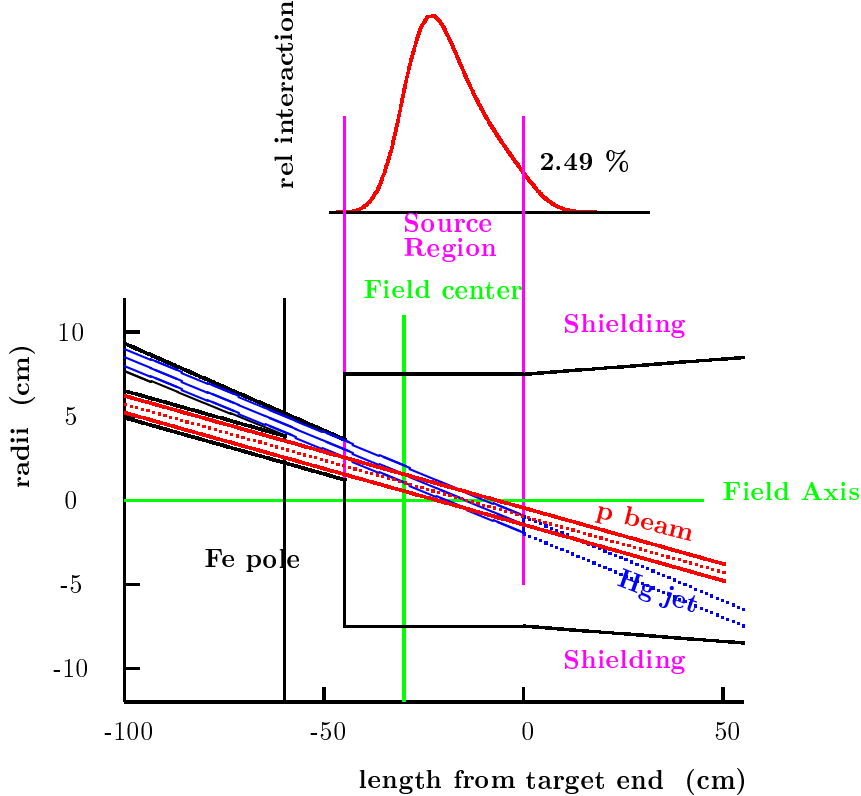
## 5 Study 2 Example

For Study 2, several parameters were changed from the above example. The jet radius was halved, the jet velocity increased, the magnetic field was kept flatter,

and the nozzle introduced inside the magnetic field.

The beam with rms radius  $\sigma_r$  intersects a mercury jet of radius  $r_o$  at an angle  $\theta_{crossing}$ . The forward velocity of the jet is  $v_o$ . The intervals between pulses is  $t$ , and it will be assumed here that after a pulse, all the mercury outside of the nozzle is dispersed. The nozzle is at  $z_{nozzel}$  with respect to the intersection of the beam and jet center lines. Consider the following parameters:

$\sigma_r$	1.5	mm
$r_o$	5	mm
$\theta_{crossing}$	33	mrad
$v_o$	30	m/sec
$t$	20	ms
$z_{nozzel}$	-375	m



Fig\*\*\*

The geometry is shown in fig\*\*\*, with the distribution of resulting interactions as a function of  $z$  is shown above. At the time of a second, or subsequent bunch, the newly established jet will extend a distance  $z_{jet} = v_o t = 0.6$  m from the nozzle. It is seen that only 2.5 % of the interactions would occur after this location, had the beam extended indefinitely. Thus there is a negligible loss from this limited jet extent.

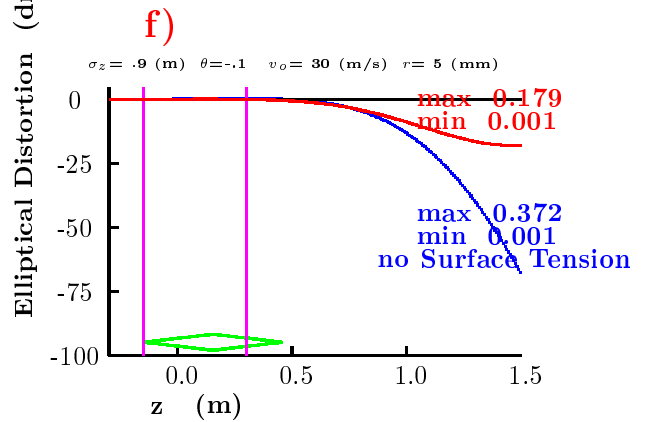
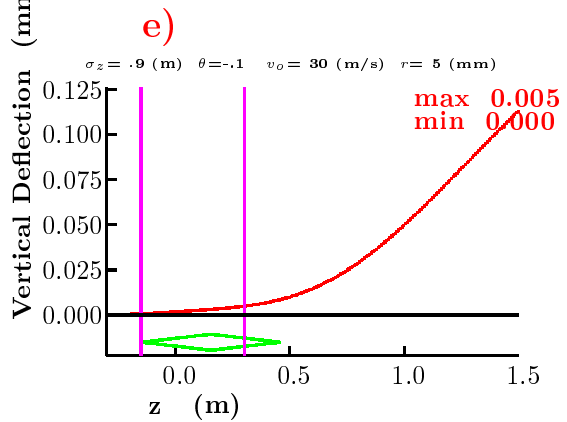
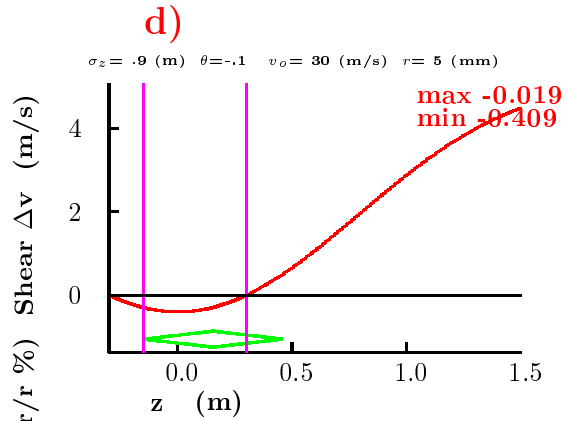
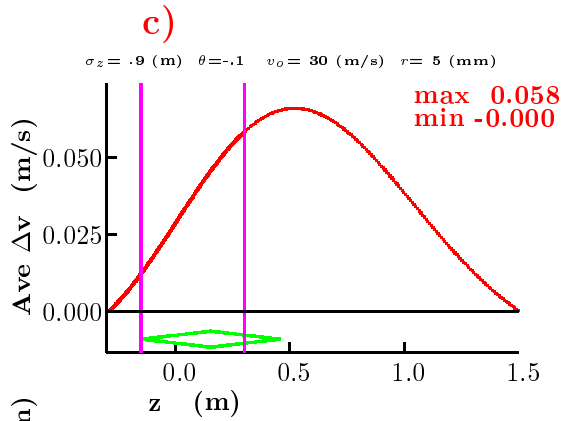
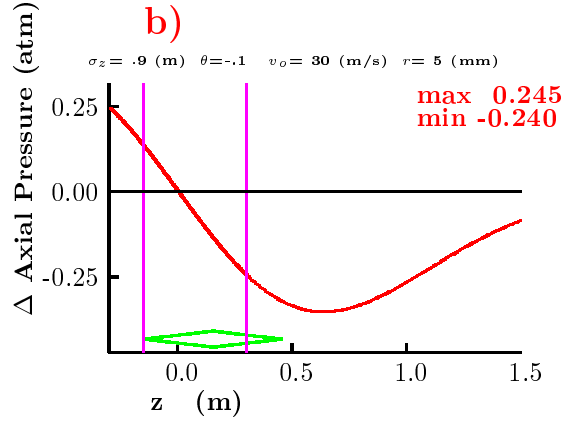
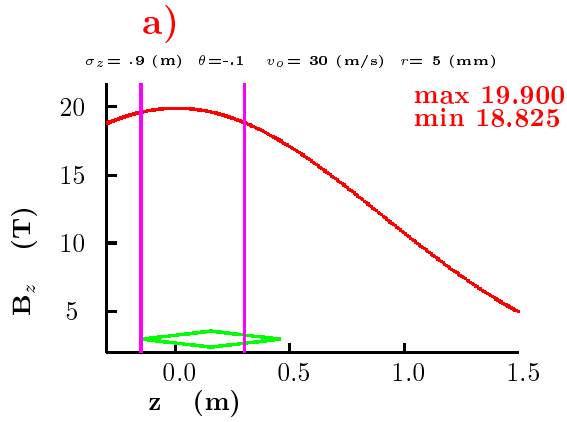
Thus the total length over which the jet must propagate without serious magnetic disruption is from the nozzle to a point 0.6 m downstream. In order to minimize the field non uniformity over this length, the magnetic center (approximate point of maximum  $B_z$  is placed at the center of this length. i.e. the magnetic center is set at a distance  $z_{magnet} = z_{jet}/2 - z_{nozzle} = -.15$  m with respect to the jet-beam intersection.

The proton beam enters at an angle  $\theta_{beam}$  with respect to the magnet axis. The jet is at an angle  $\theta_{jet} = \theta_{beam} - \theta_{crossing}$ . The vertical distance  $y_o$  from the magnet center ( $z = 0, r = 0$ ) to the jet axis at  $z = 0$  can be chosen to minimize beam disruption. We assuming a Gaussian distribution of  $B'_z$  vs  $z'$ , with a maximum value of  $B_o$ , The jet conductivity  $\kappa$ , density  $\rho$ , and surface tension  $T_{surface}$ , and the other parameters are given below:

$B_o$	20	T
$\sigma'_z$	.8	m
$\theta_{jet}$	-100	mrad
$\kappa$	$10^6$	$\Omega$ m
$\rho$	$13.5 \cdot 10^4$	$kg/m^3$
$T_{surface}$	.456	$N/m$
$p_{gas} = p_{atmospheric}$	$10^5$	$N/m^2$

The following figures shown here use a horizontal scale with  $z = 0$  at the magnetic center. Plots are shown for

- a) The axial magnetic field  $B_z$
- b) The hydrostatic pressure on the jet axis with respect to the environment outside the jet ( $p_{axis} - p_{gas}$ )
- c) The average deceleration of the jet  $\Delta_v$ (Ave)
- d) The maximum shear acceleration/deceleration of the upper/lower limits of the jet  $\Delta_v$ (shear)
- e) The vertical displacement of the jet due to deflecting forces  $y$
- f) The total transverse distorting forces  $F_{distort}$
1. The resulting elliptical distortion ( $\delta x/r = -\delta y/r$ ), without and without surface tension



We see that over the extent of the new jet (from  $- .3$  to  $.3$  m):

- The maximum axial field deviations are  $\pm 1.1$  T = 5%



- The axial pressure difference has a minimum of - 0.25 atmospheres. Thus if the jet is operating in a gas (He or Argon) at a pressure greater than or equal to .25 atmosphere, then the negative pressures will be avoided, and there will be no tendency to cavitate prior to the arrival of the beam.
- The maximum average deceleration of the jet is very small compared to the average jet velocity:  $0.06/30 \approx 0.2\%$ .
- The maximum decelerations (from shear forces) are also small compared to the average jet velocity:  $0.4/30 \approx 1.3\%$ .
- The deflections of the jet are very small:  $5 \mu\text{m}$ .
- The jet distortions ( $\Delta$  width / ave width) are approximately 0.4% without surface tension, and less than 0.2

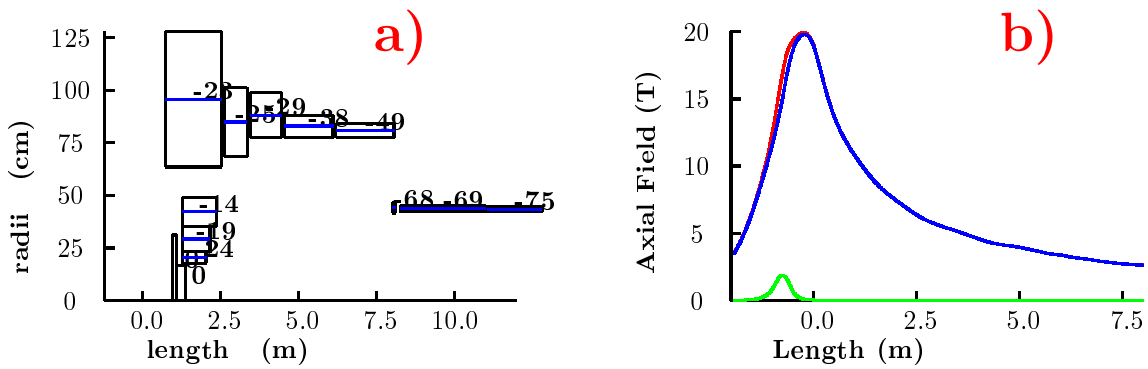
Beyond the target region ( $z=.3$  to  $1.5$  m), the effects are larger, but still not sufficient to break up the jet. The maximum shear is about 5 m/sec, and the distortion 20 %. But these numbers are probably meaningless, since the jet will have been disrupted by the beam. These results are much better than in the earlier example and are considered to be acceptable.

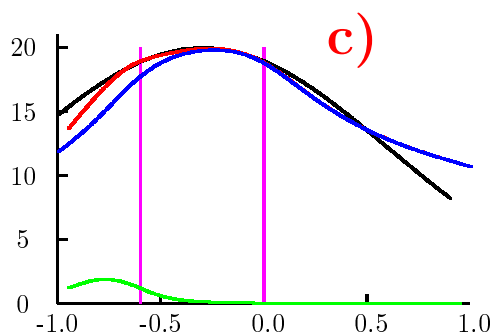
## 6 Coil Design

The coil dimensions are given in the following table and plotted in figure a.

len1 m	gap m	dl m	rad m	dr m	I/A A/mm <sup>2</sup>	n I A	n I l A m
Fe							
0.980	0.980	0.108	0.000	0.313	0.00	0.00	0.00
1.088	-.000	0.312	0.000	0.168	0.00	0.00	0.00
Hollow							
1.288	-.112	0.749	0.178	0.054	-24.37	0.98	1.26
1.288	-.749	0.877	0.231	0.122	-19.07	2.04	3.74
1.288	-.877	1.073	0.353	0.137	-14.87	2.18	5.78
SC							
0.747	-1.614	1.781	0.636	0.642	-23.39	26.77	160.95
2.628	0.100	0.729	0.686	0.325	-25.48	6.04	32.23
3.457	0.100	0.999	0.776	0.212	-29.73	6.29	34.86
4.556	0.100	1.550	0.776	0.107	-38.26	6.36	33.15
6.206	0.100	1.859	0.776	0.066	-49.39	6.02	30.59
8.000	-.065	0.103	0.416	0.051	-68.32	0.36	1.00
8.275	0.172	2.728	0.422	0.029	-69.27	5.42	14.88
11.053	0.050	1.749	0.422	0.023	-75.62	3.00	8.18
12.852	0.050	1.750	0.422	0.019	-77.37	2.61	7.09
14.652	0.050	1.749	0.422	0.017	-78.78	2.30	6.22
16.451	0.050	1.750	0.422	0.015	-79.90	2.07	5.59
18.251	0.050	2.366	0.422	0.013	-80.85	2.53	6.80

The axial fields are shown in figures b and c. The components are shown from: the use of iron (green), superconductors (blue), and the total (red). The Gaussian distribution used in the above calculations is also given in figure c (black), and is seen to be a good match to the total field over the target region (-.6 m to 0).





## 7 Conclusion

- It is not acceptable to have the jet nozzle outside the magnetic field.
- With the study 2 parameters, all disruptive effects are negligible up to the distance traveled by the jet since the last pulse.
- Even beyond this location, the disruptions are not unreasonable, and would not, of themselves disrupt the jet.
- It would probably be acceptable to shorten the high field region, if this were desired for cost reasons.

## References

- [1] <http://www.cap.bnl.gov/mumu/studyii/>
- [2] K. McDonald (Ed), *An R&D Program for Targetry and Capture at a Muon-Collider Source*, Proposal to the BNL AGS Division, p.23
- [3] R. Weggel, *Behavior of conducting solid or liquid jet moving in magnetic field: 1) Paraxial; 2) Transverse; 3) Oblique*, BNL report BNL-65611/CAP-220-Muon-98R
- [4] **Phys. Today**, Feb 2000, p.29
- [5] R. Weggel, *20 T Hybrid magnet for Study II*
- [6] K. McDonald, *Damping and Radial Pinching Effects*,  
<http://www.hep.princeton.edu/~mcdonald/mumu/target/radialpinch.ps>